Aerosol Science and Technology

ISSN: 0278-6826 (Print) 1521-7388 (Online) Journal homepage: https://www.tandfonline.com/loi/uast20

Mobility particle size spectrometers: Calibration procedures and measurement uncertainties

A. Wiedensohler, A. Wiesner, K. Weinhold, W. Birmili, M. Hermann, M. Merkel, T. Müller, S. Pfeifer, A. Schmidt, T. Tuch, F. Velarde, P. Quincey, S. Seeger & A. Nowak

To cite this article: A. Wiedensohler, A. Wiesner, K. Weinhold, W. Birmili, M. Hermann, M. Merkel, T. Müller, S. Pfeifer, A. Schmidt, T. Tuch, F. Velarde, P. Quincey, S. Seeger & A. Nowak (2018) Mobility particle size spectrometers: Calibration procedures and measurement uncertainties, Aerosol Science and Technology, 52:2, 146-164, DOI: 10.1080/02786826.2017.1387229

To link to this article: https://doi.org/10.1080/02786826.2017.1387229

Published online: 26 Oct 2017.

AEROSOL SCIENCE AND TECHNOLOGY
2018, VOL. 52, NO. 2, 146–164
https://doi.org/10.1080/02786826.2017.1387229

Mobility particle size spectrometers: Calibration procedures and measurement uncertainties

A. Wiedensohler[a], A. Wiesner[a], K. Weinhold[a], W. Birmili[a,e], M. Hermann[a], M. Merkel[a], T. Müller[a], S. Pfeifer[a], A. Schmidt[a], T. Tuch[a], F. Velarde[a,f], P. Quincey[b], S. Seeger[c], and A. Nowak[d]

[a]Leibniz Institute for Tropospheric Research, Leipzig, Germany; [b]Department of Chemical, Medical and Environmental Sciences, National Physical Laboratory, Teddington, Middlesex, United Kingdom; [c]Materials and Air Pollutants, Federal Institute for Materials Research and Testing, Berlin, Germany; [d]Aerosol and Particle Diagnostic, Physikalisch-Technische Bundesanstalt, Braunschweig, Germany; [e]German Environment Agency, Berlin, Germany; [f]Laboratory for Atmospheric Physics, Institute for Physics Research, Universidad Mayor de San Andres, La Paz, Bolivia

ABSTRACT

Mobility particle size spectrometers (MPSS) belong to the essential instruments in aerosol science that determine the particle number size distribution (PNSD) in the submicrometer size range. Following calibration procedures and target uncertainties against standards and reference instruments are suggested for a complete MPSS quality assurance program: (a) calibration of the CPC counting efficiency curve (within 5% for the plateau counting efficiency; within 1 nm for the 50% detection efficiency diameter), (b) sizing calibration of the MPSS, using a certified polystyrene latex (PSL) particle size standard at 203 nm (within 3%), (c) intercomparison of the PNSD of the MPSS (within 10% and 20% of the dN/dlogDP concentration for the particle size range 20–200 and 200–800 nm, respectively), and (d) intercomparison of the integral PNC of the MPSS (within 10%). Furthermore, following measurement uncertainties have been investigated: (a) PSL particle size standards in the range from 100 to 500 nm match within 1% after sizing calibration at 203 nm. (b) Bipolar diffusion chargers based on the radioactive nuclides Kr^{85}, Am^{241}, and Ni^{63} and a new ionizer based on corona discharge follow the recommended bipolar charge distribution, while soft X-ray-based charges may alter faster than expected. (c) The use of a positive high voltage supply show a 10% better performance than a negative one. (d) The intercomparison of the integral PNC of an MPSS against the total number concentration is still within the target uncertainty at an ambient pressure of approximately 500 hPa.

ARTICLE HISTORY
Received 6 July 2017
Accepted 26 September 2017

EDITOR
Pramod Kulkarni

1. Introduction

Mobility particle size spectrometers (MPSS) belong to the essential instruments in aerosol science that determine the particle number size distribution (PNSD) of the submicrometer aerosol particle population. Depending on the setup, MPSSs are able to determine a PNSD from typically a few nanometers to around one micrometer in particle mobility diameter. The MPSS has been widely described in the literature (e.g., ten Brink et al. 1983; Fissan et al. 1983; Kousaka et al. 1985; Winklmayr et al. 1991; Wang and Flagan 1990; Chen et al. 1998; Wiedensohler et al. 2012), often under the name scanning mobility particle sizer (SMPS) or differential mobility particle sizer (DMPS). The primary product of an MPSS measurement is an electrical particle mobility distribution, which needs to be converted to a PNSD by a numerical inversion procedure (e.g., Hoppel 1978; Pfeifer et al. 2014).

Although these MPSSs are designed to operate autonomously with minimum attention, quality assurance measures are required on a regular basis to ensure the delivery of reliable data. Comparisons between different MPSS instrument types and individuals have been reported in numerous studies (e.g., Dahmann et al. 2001; Khlystov et al. 2001; Helsper et al. 2008; Gómez-Moreno et al. 2015). Specific recommendations for a complete system of quality assurance measures, and well-founded estimates of the measurement uncertainties have, however, been missing in the literature. This article describes and discusses a complete set of quality assurance measures for MPSS instruments based on bipolar diffusion charging and a condensation particle counter (CPC) as the detector.

CONTACT A. Wiedensohler ali@tropos.de Leibniz Institute for Tropospheric Research, Permoserstr. 15, 04318 Leipzig, Germany.
Color versions of one or more of the figures in the article can be found online at www.tandfonline.com/uast.

Quality standards for PNSD measurements may differ for different applications such as atmospheric studies, laboratory investigations, workplace, or indoor exposure assessment as well as emission surveys. The atmospheric observational infrastructures WMO-GAW (*World Meteorological Organization—Global Atmosphere Watch*) and ACTRIS (*Aerosols, Clouds, and Trace gases Research InfraStructure*), as two examples, have devised a quality assurance system that requires frequent instrumental calibrations (WMO-GAW report 227; Wiedensohler et al. 2012). The European Center for Aerosol Calibration (ECAC, http://www.actris-ecac.eu) and the World Calibration Center for Aerosol Physics (WCCAP, http://wmo-gaw-wcc-aerosol-physics.org) offer such calibration services within WMO-GAW and ACTRIS. As a rule, an MPSS passes an ECAC/WCCAP calibration if (a) the sizing uncertainty against a certified particle size standard of 203 nm is ±3% or better, (b) the PNSD should be within 10% against the reference MPSS in the size range from 20 to 200 nm and 20% between 200 and 800 nm, and (c) the integrated PNC agrees within 10% with the PNC measured by an independently calibrated reference condensation particle counter (CPC).

The agreement of PNSDs measured by different MPSSs has been found to be best for the particle size range from 20 nm to 200 nm in particle mobility diameter (Wiedensohler et al. 2012). Outside this range, the deviations might be larger for a number of reasons: for particles <20 nm, the fraction of charged particles in a given bipolar charge equilibrium is low (Wiedensohler 1988) and the theoretical description of losses due to diffusion might cause elevated uncertainties. Above particle diameters of 200 nm, the larger fractions of multiply charged particles and the effect of incorrect sizing on the steep spectral slope possibly lead to an increased uncertainty. Producing a predictable bipolar charge distribution in the MPSS instrument is one of the prerequisites for an accurate data inversion.

To achieve the highest accuracy with an MPSS measurement, it is also necessary to test the above-described main technical components individually, i.e., (a) the optional *preimpactor* (separating large particles), (b) the *bipolar diffusion charger*, (c) the *differential mobility analyzer* (DMA), and (d) the CPC. To evaluate the performance, the following quality assurance procedures (Figure 1) are proposed, based on our laboratory-based experience at the ECAC/WCCAP:

a) calibration of the size-dependent counting efficiency curves of the reference CPC and candidate CPC (as part of the candidate MPSS) by a traceable chain of particle number concentration to the SI (Système international d'unités) using a calibrated FCAE against primary standards for voltage, current, time, and mass flow
b) calibration of the sizing of the DMA set-up by employing a certified particle standard such as PSL
c) intercomparison of the candidate MPSS against a reference MPSS
d) intercomparison of the integrated PNC of the candidate MPSS against the direct PNC measurement of a reference CPC

Using a preimpactor ensures that the measured PNSD will be physically limited at the cut-off diameter. This improves the accuracy of the multiple charge inversion used to derive the PNSD. The use of the impactor might not be essential in situations where there is no significant PNC above the size range to be measured. In the atmosphere, for example, the number concentration of particles larger than 800 nm is often very low, so a preimpactor might not be needed. However, the

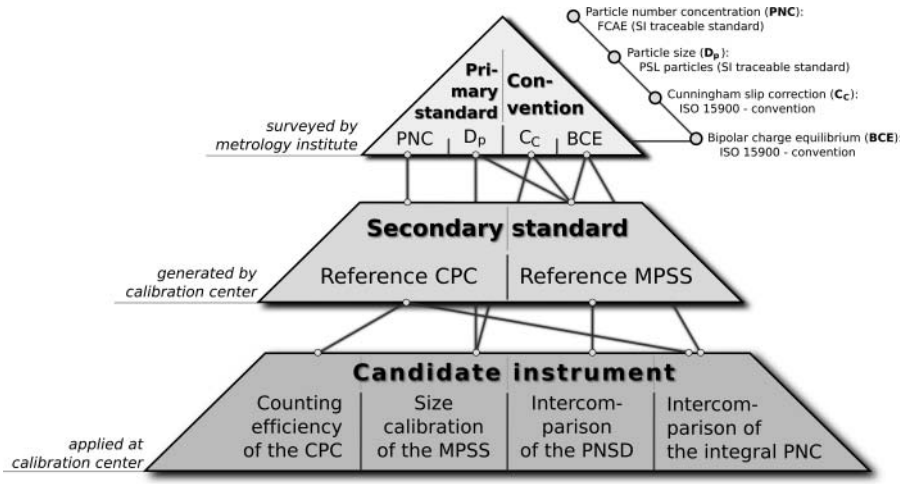

Figure 1. Traceability of MPSS measurements to a set of certified standards and conventions. To facilitate the time-efficient calibration of candidate instruments, intermediate standards (so-called "reference instruments") are used at the calibration center.

preimpactor is strongly recommended if there is a significant source of course particles such as mineral dust or sea spray.

Prior to their electrical mobility classification, the aerosol particle population has to undergo a bipolar charging process, because carrying at least one charge is a prerequisite for particles to be separated in an electric field. One class of bipolar diffusion chargers work on the basis of the ionization of air molecules by radioactive material that creates a cloud of both positive and negative ion clusters. Commonly used radioactive sources are Kr^{85}, Am^{241}, Po^{210}, or Ni^{63}. Ideally, the entire particle population will reach a bipolar charge distribution, which, for example, can be calculated based on the charging theory by Fuchs (1963) and assumptions on the mobility and mass of the positive and negative ion clusters. Wiedensohler (1988) introduced a parameterization of this bipolar charge distribution based on fitted experimental data. It is theoretically independent of ambient pressure at room temperature and therefore assumed valid for PNSD measurements performed in a tempered room. The bipolar charge equilibrium is based on the ratio of the mobility of positive and negative air ions, which would change in the same manner, if the pressure changes (Fuchs 1963). The bipolar charge distribution is widely used in commercial and custom-designed instrument softwares and recommended by convention as a computation basis in the standard ISO 15900 (https://www.iso.org/standard/39573.html) for the entire submicrometer particle size range. There are also alternative bipolar diffusion chargers. The ionizer uses positive and negative ions produced by corona discharge, resulting in a bipolar charge distribution similar to ISO 15900, according to the manufacturer. The bipolar charging by soft X-rays produces a different bipolar charge distribution, which was determined and parameterized by Tigges et al. (2015).

The advantage of bipolar diffusion charging is a relative independence from the PNC and the aerosol flow rate, as long as the equilibrium number concentration of ion pairs is sufficiently higher than the PNC as well as the aerosol flow is limited to few l/min. Since the typical equilibrium ion pair concentration is approximately 10^7 cm^{-3}, the PNC should not exceed 10^6 cm^{-3}. The calculated bipolar charge distribution may have a reduced accuracy due to

a) the very low charging efficiency for particles smaller than 20 nm, which have a large fraction of uncharged particles,
b) increasing fractions of multiply charged particles for the particle size ranges greater than 200 nm, and
c) the charging state of the aerosol particles before entering the charger, for example, any extreme unipolar charging.

Calculations cover charging states from −10 to +10 elementary charges (including zero charge), the fractions strongly depending the excess of air ions and on the particle size, especially if the particle surface area concentration is high due to a pronounced accumulation mode.

A DMA (see, e.g., Knutson and Whitby 1975; Liu and Pui 1974; Flagan 1999; Stolzenburg and McMurry 2008) is usually designed as a cylindrical capacitor in which charged aerosol is injected through an annular slit close to the outer electrode and merged with the particle-free and dried sheath air flow.

A DMA separates the particles according to their electrical mobility Z_p, which is a function of particle charge ($n_e^* e$), particle diameter D_p, the corresponding Cunningham slip correction C_C and the gas viscosity η:

$$Z_p = \frac{u_e}{E} = n_e \cdot e \cdot \frac{C_C}{3\pi \cdot \eta \cdot D_p}$$

It is important to note that the Cunningham slip correction is based on empirical evidence and conventional values for it are given in ISO 15900 (see also Wiedensohler et al. 2012). If the geometry and size of the DMA and its operational parameters such as sheath flow and sample flow are known, one can calculate and adjust the voltage between the electrodes needed to let the fraction of charged particles with the target electrical mobility pass through the DMA from the entrance to the annular exit slit in the central rod of the capacitor. The "DMA transfer function" (Birmili et al. 1997; Collins et al. 2002; Hagwood et al. 1999; Knutson and Whitby 1975; Russell et al. 1995; Stolzenburg 1988; Zhang and Flagan 1996) can be described as a triangle selecting a range of electrical mobilities with an averaged transfer probability of 50%. In reality, the transfer function differs slightly from a triangle and the transfer probability decreases with decreasing particle diameter. Particle losses within a DMA, including a nonideal transfer function, can however be accounted for by using the method of "equivalent length", as described in Wiedensohler et al. (2012). This particle loss correction then only depends on the DMA type and the aerosol flow rate. Possible malfunctions of a DMA could occur due to internal aerosol particle deposition, flow or electric field disturbances, arcing, or mishandling during disassembly/reassembly. This is especially a problem if these nonidealities lead to a broadening of the transfer function.

Particles within a small electrical particle mobility bandwidth pass through the DMA and their number concentration is measured by the CPC (see, e.g., Agarwal and Sem 1980; Stolzenburg and McMurry 1991; Wiedensohler et al. 1997; Hermann et al. 2007; Tuch et al. 2016). Small particles with diameters below approximately 100 nm need magnification to a size, which can be

detected optically in the CPC. In a regular butanol-based conductive cooling CPC, the aerosol flow is slightly heated and then saturated with butanol vapor. In a cooling section (also called the condenser), the butanol vapor becomes supersaturated and condenses onto the particles, forming droplets of approximately 10 μm. These droplets are led through a focusing nozzle and then counted individually by a laser optic. From the droplet counting frequency, counting interval duration, and the aerosol flow rate, the time resolved PNC can be calculated with a time resolution of typically 1 s. The lower detection efficiency diameter is determined by the Kelvin diameter of the particles, which is a function of the physical diameter and the chemical affinity between the particle and the butanol, and can be varied by changing the temperature difference between the saturator and the cooling section. The chemical affinity is dependent on the particles surface properties and hence the CPC detection efficiency is – especially at lower sizes—particle material dependent. This material dependency is however rather small if butanol is used as working fluid and the temperature difference between saturator and condenser is optimized to reach a specific D_{P50}.

Malfunctions may occur if (a) the saturation process is not at optimum, (b) the temperature difference is not stable, (c) droplets are lost by impaction on the edges of the focusing nozzle, (d) the particle beam is outside the laser focus, or (e) the nominal flow rate is not reached. Manufacturers give uncertainties of up to 10% to the measured PNC. In reality, however, it is only a few percent if the instrument is technically performing well.

2. Calibration procedures

The calibration procedures mentioned above have been implemented at ECAC/WCCAP for instruments used in atmospheric aerosol measurements, and are here described in detail. The calibration procedures are, however, also suitable for other applications. Calibration of an MPSS should ideally be done at a calibration center with international reputation, which meets the requirements of the ISO standards or atmospheric observational networks, especially SI-traceability, and providing one or more regularly maintained and calibrated reference MPSSs and CPCs. However, calibrations can be performed at measurement stations. These calibrations can include the PSL sizing and a reference CPC and MPSS as comparison instruments, which have been calibrated before in the laboratory.

The determination of size-dependent CPC counting efficiency curves and the sizing of the DMA setup (at the scale of the PSL particles) are traceable calibrations, because they can be traced back to SI units. The sizing for particles smaller than the certified PSL particle size calibration depends on the Cunningham slip correction and thus on its uncertainty. The intercomparisons of PNSDs against each other, as well as the integrated PNC against the reference CPC are based on "black box" approaches, because the bipolar charge distribution, Cunningham slip correction, and diffusion loss correction used in the data inversion are conventions and are not traceable. While the intercomparison of the PNSDs of the candidate and the reference MPSSs only provides a qualitative result (the PNSD is principally not traceable), a quantitative performance measure is given by the intercomparison of the integrated PNC of the candidate MPSS against the directly measured PNC of the reference CPC. Preferably, the CPCs should have the same D_{P50}.

MPSS-based calibrations at the ECAC/WCCAP are usually done with atmospheric aerosols. This procedure has two main reasons:

1. The atmospheric aerosol is already naturally precharged, but with an unknown nonequilibrium bipolar charge distribution. When using a bipolar diffusion charger, there is a high probability of obtaining a bipolar charge distribution corresponding close to the ideal equilibrium.
2. A unipolar precharged laboratory-generated aerosol needs more interaction with gas ions to be brought into a bipolar charge equilibrium, e.g., by using a bipolar charger with a sufficient activity. However, if the equilibrium is not reached, the calculations of PNSDs and PNCs based on the multiple charge corrections will be inaccurate. This would lead to an invalid intercomparison.

Results from several ECAC/WCCAP calibration workshops are shown to demonstrate the different steps of the calibration procedure. These results are for illustrative purposes, and the research institutions of the candidate instruments have been anonymized in the legends of the different figures.

2.1. Calibration of condensation particle counters

2.1.1. Traceability of the reference particle counter

The CPC used to measure the PNC is calibrated against a reference FCAE. A FCAE consists of an electrically conducting and grounded cup as a guard to cover the sensing element that includes a conducting high efficiency aerosol filter (not necessarily conductive) to capture aerosol particles, an electrical connection between the sensing element and an electrometer circuit, and a flow meter. The capture efficiency for a FCAE is expected to be greater than 98 % for particles above 5 nm and sample flows above 1 l/min. The main challenge is that particles might get lost by diffusion before entering the cup and

then are not detected. FCAEs measure very small electrical currents down to the femto Ampere range, or respectively, electrical charge densities as small as 10^{-15} Coulomb/cm3; and the signal to noise ratio is the limiting factor. FCAEs used for calibration purposes must—according to ISO 27891:2015—have a stable zero baseline, i.e., the zero-corrected absolute arithmetic mean electric current when no particles are present must be less than 1 fA (femto-ampere) with a standard deviation below 0.5 fA. If, for example, singly charged particles with a PNC of 1000 cm^{-}3; are measured, the corresponding electrical current reading of an FCAE at 1 l/min sample flow would then be 2.67 fA with a relative uncertainty of at least ± 20% (according to an absolute uncertainty of at least ± 0.5 fA). A comprehensive comparison of FCAE measurements found about ± 5% relative deviation (deviation of the means) among eight FCAEs with 1 l/min sample flow. The uncertainties in this test were up to 20% (Hogström et al. 2014). Although uncertainties are expected to increase at smaller particle sizes and lower concentrations, the results provided experimental evidence that the requirements of the ISO standard can practically be met.

The ECAC/WCCAP reference FCAE is SI-calibrated against a femto-Ampere source at the German national metrology institute (PTB—Physikalisch-Technische Bundesanstalt, Braunschweig) The reference CPC of the ECAC/WCCAP is twice per year calibrated against the reference aerosol electrometer using singly charged monodisperse silver particles.

Figure 2 shows the ECAC/WCCAP CPC calibration set-up previously described in Tuch et al. (2016). The generation of the monodisperse calibration aerosol is briefly described in the following paragraph. Silver is evaporated in a N_2 carrier gas flow through a tube furnace aerosol generator (Scheibel and Porstendörfer 1983). In the cooling section, supersaturated silver vapor nucleates to primary particles a few nanometers in diameter. The nucleation process and the subsequent agglomeration of the silver particles are then quenched by an additional N_2 flow. Afterward, the silver particle agglomerates are annealed at 450°C by passing through a second tube furnace and solidify as nearly spherical particles at the exit. The silver particles are then charged in a bipolar diffusion charger. Monodisperse calibration aerosols in the size range of 3–40 nm can then be selected by using a Nano-DMA setup. The size resolution in a DMA is influenced by the sheath to sample airflow ratio but also by diffusion broadening. At high ratios, e.g., 20:1, the transmitted particle fraction is highly monodisperse with a typical geometric standard deviation (GSD) well below 1.1. This ratio should be high (a) to minimize the non-diffusive width of the transfer function and (b) to minimize the contribution of diffusional broadening to the transfer function. Finally, the test aerosol is diluted with particle-free room air in a mixing chamber to adjust the PNC and to provide sufficient flow rate for all instruments.

The linearity calibration is done with 40 nm monodisperse particles as shown in Figure 3. A 1:1 slope demonstrates an asymptotic counting efficiency of 100% (also called plateau efficiency). We use a particle size of 40 nm, because the CPC TSI model 3772 operates at the plateau counting efficiency.

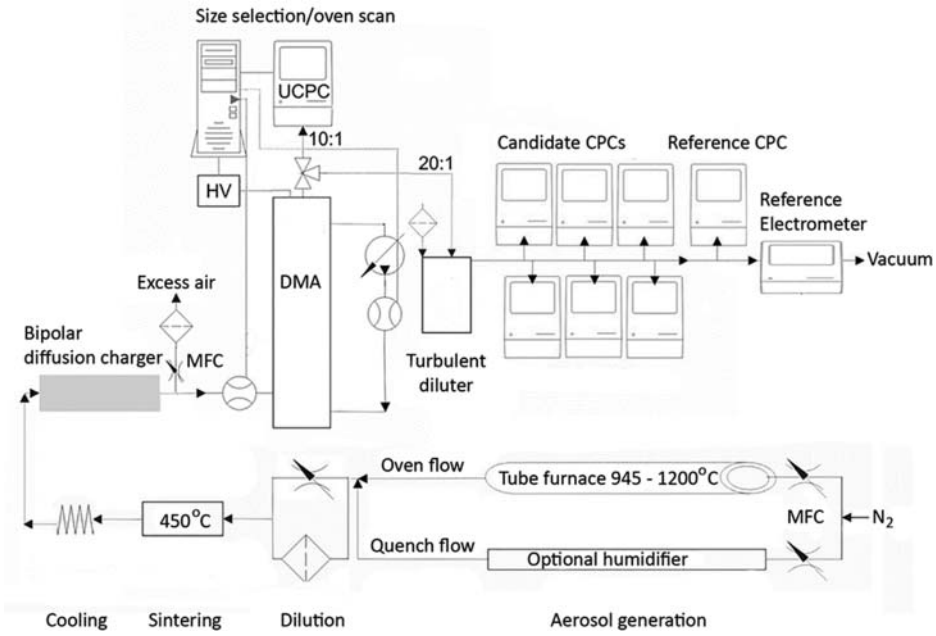

Figure 2. CPC calibration setup used at ECAC/WCCAP.

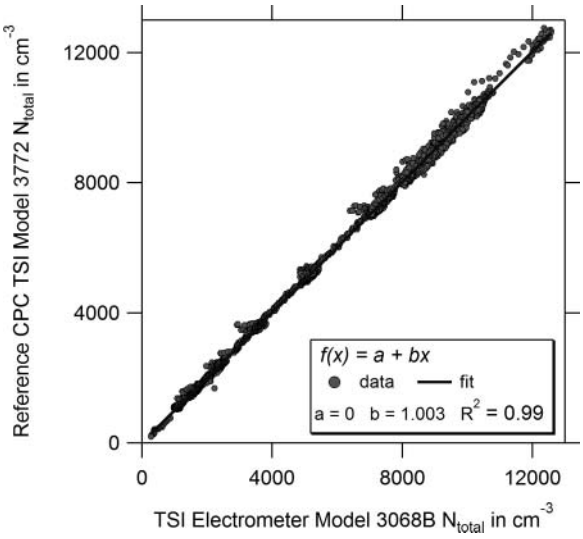

Figure 3. Calibration of the ECAC/WCCAP reference CPC model 3772 (coincidence-corrected) against the reference aerosol electrometer model TSI model 3068B. Data are plotted at a time resolution of 1 s.

2.1.2. Calibration of candidate condensation particle counters

A successful CPC calibration in terms of the CPC counting efficiency curve and the D_{P50} is a prerequisite for evaluating the performance of an MPSS. The following steps have to be considered, taking a regular CPC TSI model 3772 as an example:

1. Initial status check without any maintenance to obtain the status of the candidate CPC.
   a. Measuring the exact CPC aerosol flow rate, which is allowed to deviate up to 3% from the nominal 1 l/min. The exact flow rate should be used in the calculation of the counting efficiency
   b. Checking the CPC counting efficiency curve. If necessary, the candidate instrument will then go through maintenance
2. Maintenance of the candidate CPC:
   a. Cleaning of the saturator wick or, alternatively, replacing it with a new one (this can be done by the user on a regular schedule)
   b. Cleaning of the aerosol nozzle that focuses the droplet flow into the optics (this can be done by the user on a regular schedule)
   c. Cleaning of the critical orifice that ensures a constant aerosol flow rate (this can be done by the user on a regular schedule)
   d. Cleaning the optics, if necessary (this can be only done by an experienced person)
   e. Measuring the actual flow rate again
3. Final calibration after maintenance of the candidate CPC

For the CPC calibration of the detection efficiency curve, the particle number concentration of the monodisperse silver particles should be in the range of 1000–5000 cm^{-3} to avoid coincidence in the measuring volume of the CPC optics, and to reach a sufficient number concentration for the aerosol electrometer measurement. At WCCAP/ECAC, we use an electrometer flow rate of 4 l/min, decreasing the lower detection limit to approximately 200 cm^{-3} for acceptable accuracy and signal to noise ratio of the current. Monodisperse particles are generated in the range 5–40 nm and the counting efficiency is calculated, taking into account:

a) the measured aerosol flow rate
b) the number of particle counts at the digital CPC pulse out
c) the counting time
d) the PNC derived from the electrometer

To evaluate the calibration results, following targets are considered.

a) The plateau efficiency should not deviate more than 5% from the reference CPC (manufacturers normally indicate an uncertainty up to 10%).
b) The lower counting efficiency diameter of the CPC 3772 for silver particles normally ranges from 7 to 9 nm as shown in Tuch et al. (2016) (the manufacturer gives the value of 10 nm).

The performance of a CPC can be evaluated by using a best fit to a function that describes the steep part of the detection efficiency curve. As an example, Figure 4 shows the CPC counting efficiency curves of an initial and final calibration. The theoretical fit function from Stolzenburg and McMurry (1991) is also given in the figure and was used for data interpretation. The fit parameters are the plateau efficiency A [dimensionless], the lower detection limit B [nm] and D_{P50}, C [nm]; the particle diameter is denoted by x.

In this example, the CPC was cleaned after the initial check. Note that the counting efficiency curve and the lower detection efficiency diameter of the reference CPC are determined during the calibration workshops in parallel.

2.1.3. Uncertainty in CPC efficiency calibration

For the determination of the CPC detection efficiency, a detailed methodology is described in ISO 27891:2015. The main difference to the setup in Figure 2 is that the monodisperse test aerosol is split into only two equivalent partial flows and the PNC is measured in parallel by only one candidate CPC and a reference FCAE. While methodology and outcome are in principle the same in both cases, the ISO standard has an elaborated concept for the estimation of uncertainties in the determination of the candidate CPC's detection efficiency. Due to the

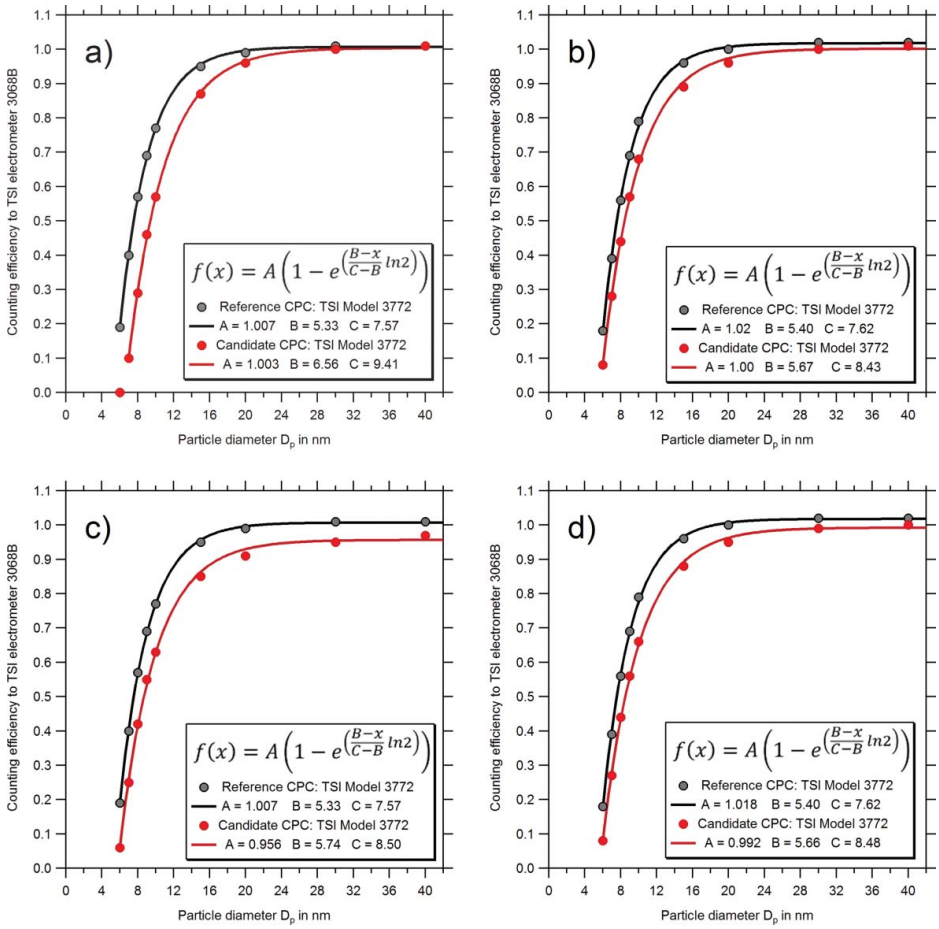

Figure 4. Example of CPC counting efficiency curves of the initial and final calibration after maintenance. The upper two figures show the initial (a) and final (b) calibration of a case when D_{P50} was not within the target range of 7–9 nm, while the lower two figures show an example when the target plateau efficiency was not reached during the initial calibration (c) but was reached after maintenance and successful adjustment (d). (An counting efficiency of 1 corresponds to 100%.)

complexity of the experimental setup and the calibration procedure itself, straightforward error propagation is not feasible and the combined relative standard uncertainty in the detection efficiency is the result of several type A (repetition and statistical treatment) and type B (other means) uncertainty components. The following uncertainty components are considered:

a) FCAE detection efficiency: The corresponding type B uncertainty is usually evaluated by a national metrology institute on a regular basis. Values are expected to be below 1%.
b) FCAE and CPC flow rates and their uncertainties are evaluated case-by-case by repeated comparison to a calibrated SI-traceable mass flowmeter. Uncertainties are most likely below 2%.
c) Uncertainty in multiple charge correction: Depending on the test aerosol generation and the size of the particles, the FCAE raw data have to be corrected for multiply charged particles before conversion into PNC. A case-by-case evaluation is unavoidable and can be determined semiempirically in the plateau region. The uncertainty is in all probability few % depending on the selected monodisperse diameter.
d) Splitter bias: A case-by-case evaluation quantifies a possible misbalance of the PNCs in the partial flows by repeated measurements. The bias factor should be within the 0.95–1.05 interval. The relative uncertainty is usually very small (below 1%).
e) Repeatability of the efficiency determination: This component is evaluated case-by-case through short-term repetitions. Values below 1% are expected.
f) Uncertainty contribution from test particle size uncertainty: This component has an effect in the steep region where the CPC detection efficiency is significantly size dependent. It is the product of the relative size uncertainty and the slope of the efficiency curve, which itself is the target of the calibration. The uncertainty of the DMA-selected

particle size results from the calibration with certified monodisperse test particle standard or a DMA calibrated according to ISO 15900:2009, trusting the Cunningham correction factor. The width of the monodisperse particle size bin is then dependent on the aerosol flow to sheath flow rate and the diffusion broadening.

According to these estimations, the combined relative standard uncertainty in the detection efficiency of CPCs seems to be below 10% in most cases.

2.2. Calibration of mobility particle size spectrometers

A complete calibration of a candidate MPSS is complex and requires the following steps:

a) Set-up of the candidate MPSS to the configuration as it is usually operated at the observatory or laboratory
b) Set-up of the reference MPSS and CPC parallel to the candidate MPSS
c) Initial intercomparison run of the candidate MPSS and the reference MPSS and the reference CPC for the total particle number concentration for at least 8 h to obtain statistically relevant results
d) Evaluation of the results of the intercomparison of the PNSDs and the intercomparison of PNCs
e) Calibration of the candidate CPC of the MPSS against the reference aerosol electrometer or reference CPC as described above
f) Calibration of the sizing of the candidate MPSS with certified particle PSL size standards with a high size resolution
g) If necessary, solving technical problems of the candidate MPSS, which cause deviations from the reference instruments that are larger than the target uncertainty values
h) Final intercomparison run of the candidate MPSS and the reference MPSS against the reference CPC for the total particle number concentration for at least 8 h. Intercomparison of the PNSDs (candidate MPSS vs. reference MPSS) and PNC (integrated candidate MPSS vs. reference CPC)
i) Confirmation of a successful or a non-successful calibration in terms of a detailed report

The ECAC/WCCAP reference MPSS was described in Wiedensohler et al. (2012). ECAC/WCCAP currently provides five such reference instruments for calibrations. Their main components are a bipolar diffusion charger, using a Kr^{85} 370 MBq radioactive source, a Hauke-type DMA (Winklmayr et al. 1991) with a 28 cm long electrode, and a CPC model TSI 3772. The measured PNSD covers the range from 10 to 800 nm in mobility diameter. No preimpactor is used during the calibration experiments, since the concentration of particles larger than 800 nm is negligible in ambient air at ECAC/WCCAP, which represents an urban background aerosol population.

In the next sections, the different calibration steps are explained in detail, showing examples of results.

2.2.1. Sizing calibration and adjustment

At the ECAC/WCCAP, PSL (polystyrene latex) particles (spheres) with a certified diameter of 203 nm are used for the sizing calibration. The reasons are:

a) The number concentration of 203 nm PSL particles is still sufficiently high in a dilute suspension (one "drop" of PSL particle solution (1% by volume) in 150 ml purified water) to measure a statistically relevant number concentration peak.
b) The layer of residual material from the aqueous solution on the PSL particles after drying is not significant for PSL particles larger then 100 nm.

We consider the test at a single PSL size (203 nm) as sufficient. Experimental tests that justify this decision are supplied later in Section 3.1.1. The sizing calibration contains the following steps:

a) The initial calibration is done with PSL particles of 203 nm nominal size. The initial calibration is successful, if the geometric mean diameter of the main peak recorded by the candidate MPSS operated as normal, is within 3% of the certified PSL particle size (197 to 209 nm).
b) The initial calibration is not successful, if the measured peak diameter deviates more than 3% from the nominal PSL particle size. According to our experience, in this case the best practice is to adjust the sheath air so that the correct size classification is achieved. The most likely cause of the error is that the sheath airflow rate has changed with time due to a shift of the flow meter. An adjustment of the "effective length" in the calculation of the DMA-voltage is not considered suitable, since the geometry of the DMA is rather accurate and well known. However, if the deviation is higher than 10%, other causes of the error should be considered.
c) In the final calibration, it is again checked whether the main peak is within 3% of the nominal PSL particle size of 203 nm.

For the sizing calibration, we scan the particle size range from 100 to 400 nm with a high size resolution (up and down scans are typically approximately 4 min each) to be able to quantify the peak diameter. The up and down scan have to overlap correctly, otherwise the delay time is wrong for of an MPSS in scanning mode operation.

Figure 5 shows an example of the PSL particle calibration of a candidate MPSS. The curves show four maxima, which are:

a) the main peak at the nominal PSL particle size of 203 nm for singly charged particles
b) the first peak to the left of the nominal diameter (at 131 nm) represents doubly charged particles of 203 nm
c) the second peak to the left of the nominal diameter (at 103 nm) represents triply charged particles of 203 nm
d) the low, broad peak to the right of the nominal diameter represents doublets or triplets (agglomeration of two or three PSL particles)

The red curve is the initial PSL calibration, while the black curve shows the final sizing calibration after a successful adjustment of the sheath flow rate.

Because the majority of commercial and custom-designed MPSSs are operated in scanning mode, we suggest to measure the electrical particle mobility distribution with a high size resolution to obtain more than 20 data points for the main PSL peak. The evaluation of the peak diameter can then be done by fitting a normal function through the data points (see also Figure 5 solid line). This assures a high precision of the sizing calibration.

2.2.2. Intercomparison of particle number concentrations and size distributions

During the intercomparison of the candidate MPSS against the reference MPSS and reference CPC, the instruments are connected to a common manifold, sampling ambient aerosol. To obtain a sufficient counting statistic, the initial and final intercomparison runs are done for at least 8 h, respectively. To avoid misinterpretations, periods with a clear nucleation mode are excluded from the analysis. The particle number size distributions have been calculated using the bipolar charge distribution given in ISO15900, based on the parameterization in Wiedensohler (1988).

For a successful intercomparison, the PNSD of the candidate MPSS needs to diverge no more than +/−10% against the reference MPSS over the size range 20–200 nm. An example PNSD intercomparison is shown in Figure 6. The candidate MPSS is represented by the red curve and the reference instrument by the black curve.

In the second step of a successful calibration, the PNC of the reference CPC is intercompared against the integrated PNC of the reference and candidate MPSS as shown in the scatter plots of Figures 7a and b. The slope is close to one in both cases and is thus within the target range from 0.9 to 1.1.

2.2.3. Example of a scheduled ECAC/WCCAP MPSS intercomparison workshop

In this section, we illustrate how MPSSs of atmospheric observatories generally perform during a scheduled ECAC/WCCAP MPSS intercomparison workshop. As mentioned above, it is important to schedule regular calibrations of MPSSs to assure a high data quality with known uncertainties.

Figures 8a and b show the PNSDs of all candidate MPSSs against the reference MPSS (black line) of the initial and final calibration run (each approximately 8 h in total), respectively. For this workshop, it can be concluded that the candidate MPSSs performed generally rather well during the initial calibration run (Figure 8a). Only one MPSS was outside the target uncertainty range of

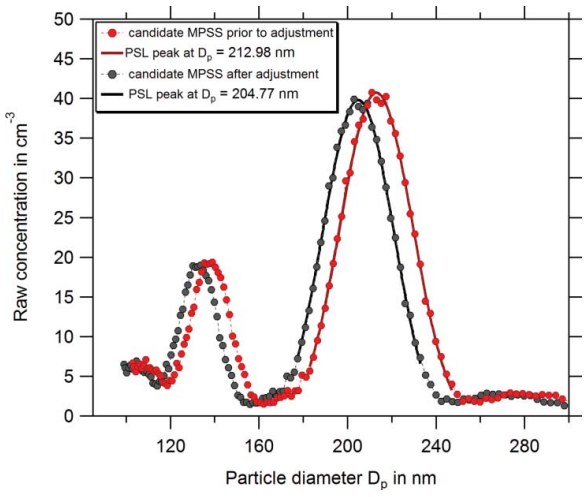

Figure 5. Calibrations of the sizing of the MPSS DMA using PSL particles with a nominal diameter of 203 nm. The example shows the initial and final PSL calibration of a candidate MPSS. The red curve is the initial PSL calibration, while the black curve shows the final sizing calibration after a successful adjustment of the sheath flow rate.

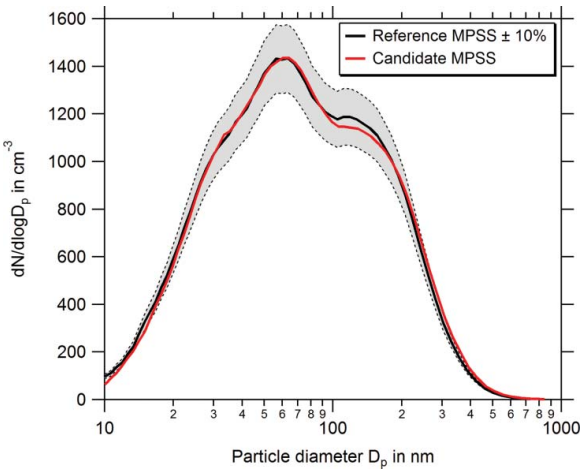

Figure 6. Successful intercomparison of the PNSD of the candidate (dark gray [red] curve) against the reference MPSS (black curve). The PNSD of the candidate MPSS is within 10% against the reference over a wide size range. The comparison was done for periods when no nucleation mode have been present.

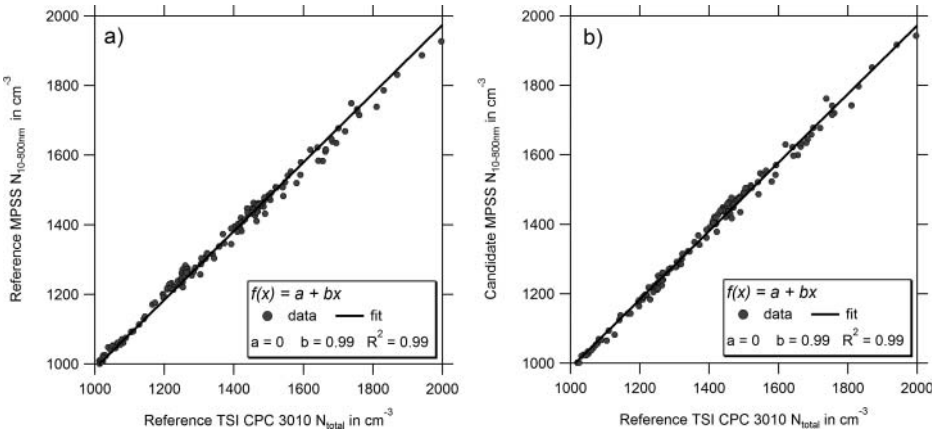

Figure 7. Intercomparisons of the reference CPC PNC against the integrated PNC of the reference and candidate MPSS as shown in (a) and (b), respectively. The slope and R^2 are close to one in both cases. The PNC have been determined for the same period as the PNSD measurement.

+/−10% (dashed lines) compared to the reference MPSS. After several maintenance steps, all candidate MPSSs were clearly within the target uncertainty range during the final calibration run (Figure 8b). These results demonstrate that MPSSs generally perform well, if the users are well trained to operate the instruments. However, it was also demonstrated that regular intercomparisons help to identify technical problems and to improve performance, even if an instrument has already been operated at a skillful level.

3. Measurement uncertainties

3.1. Sizing accuracy

3.1.1. Sizing accuracy for other PSL particle size standards

For validation purposes, we also performed additional sizing accuracy tests to confirm that a calibration with 200 nm PSL particles is sufficient. After the calibration with 200 nm PSL particles, we determined the sizing accuracy also for PSL particles with nominal diameters of 125, 350, and 500 nm without any further adjustment of the DMA sheath airflow rate. Figures 9a–d show the geometric mean diameters of the main peaks by fitting a lognormal function through the data points. The retrieved geometric mean diameters match the certified PSL particle sizes within 1%.

3.1.2. Impact of the target sizing uncertainty

For a successful intercomparison, the PNSD of the candidate MPSS needs to be within the 10% target uncertainty of the $dN/dlogD_P$ concentration against the reference MPSS. An example intercomparison of the PNSD is shown in Figure 10a. The candidate is represented by the red curve and the reference by the black curve. Both MPSS have been calibrated with a 203 nm PSL particle size standard. The peak diameter of the candidate PNSD was shifted toward a larger particle size by approximately

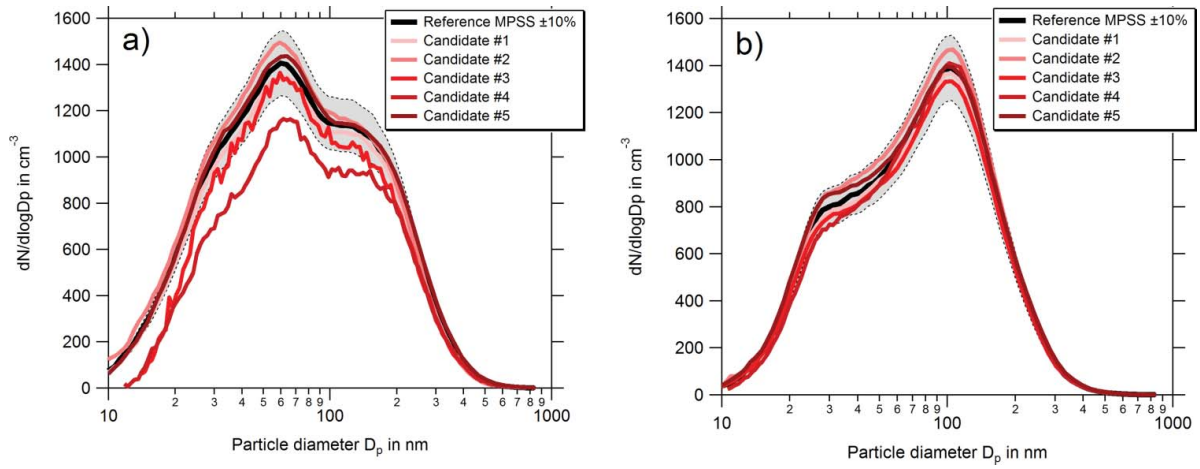

Figure 8. Example of a calibration of PNSDs of candidate MPSSs against the reference, before (a) and after (b) the adjustment. The black line represents the reference MPSS, while the dashed lines cover the target +/−10% uncertainty range.

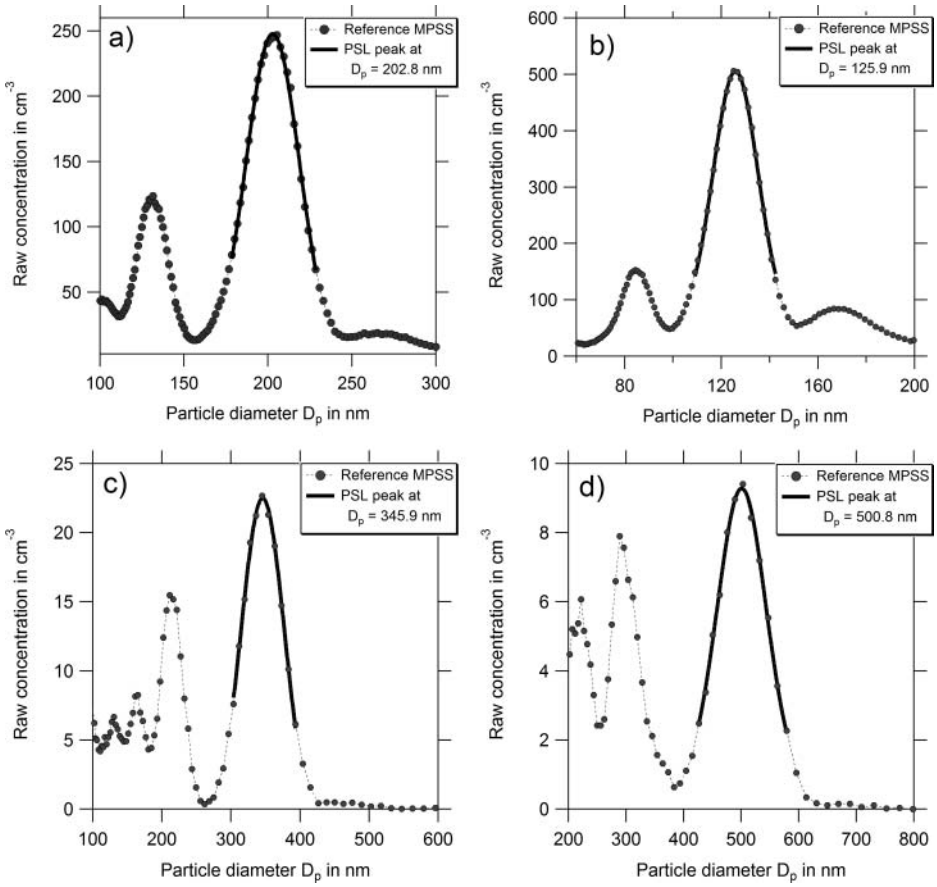

Figure 9. Calibration of the sizing of the DMA using PSL particles. (a) Calibration and adjustment with a nominal diameter of 200 nm (certified mean peak 203+/−5 nm). (b–d) Calibration with nominal diameters of 125, 350, and 500 nm (certified mean peaks: 125 +/−3 nm, 350 +/−6 nm, and 498 +/−9 nm).

3%, which would be still within the target uncertainty. This shift leads however to a disagreement above 200 nm of the $dN/dlogD_P$ concentration of more than 10% caused by the steep slope of the atmospheric PNSD. As shown in Figure 10b, the candidate MPSS would be again within the 10% target uncertainty range of the reference instrument above 200 nm if the PNSD was moved 4% in diameter toward smaller particle sizes. This result implies that an increased uncertainty of +/−20% from 200 to 800 nm should be accepted for the calibration, using the atmospheric aerosol.

3.2. Different bipolar diffusion chargers

3.2.1. Radioactive nuclides

The bipolar diffusion charger must create the expected particle charge distribution for the PNSD to be correct. We applied bipolar diffusion chargers with different radioactive nuclides (Kr^{85} 370 MBq, Am^{241} 74 MBq, and Ni^{63} 95 MBq) source to test whether the PNSDs showed deviations greater than 10%, compared to the same MPSS using a second Kr^{85} (370 MBq) as a reference, for an ambient air sample.

In our laboratory setup, we used a reference MPSS and a reference CPC. PNSD scans with ambient air were done with a time resolution of 5 min. After each scan, the MPSS and CPC inlet aerosol flows were switched between the reference and the candidate bipolar diffusion charger. The total run time was at least 8 h for each pair of bipolar diffusion chargers. For the calculation of the PNSD, we used the following settings within the inversion routine:

a) the bipolar charge distribution described in Wiedensohler (1988) and ISO 15900 for bipolar diffusion chargers using radioactive nuclides
b) the method of equivalent length as described in Wiedensohler et al. (2012) to correct for internal losses by diffusion

The results of all runs are shown in Figure 11 (Kr^{85} – Kr^{85}), Figure 12 (Kr^{85} – Am^{241}), and Figure 13 (Kr^{85} – Ni^{63}). For the atmospheric aerosol sample used, there are no deviations greater than the target value of 10%, between either the integrated PNCs or the size distributions. The radioactive chargers (Kr^{85} 370 MBq, Am^{241} 74 MBq, and Ni^{63} 95 MBq are thus equally suited to be used in an MPSS.

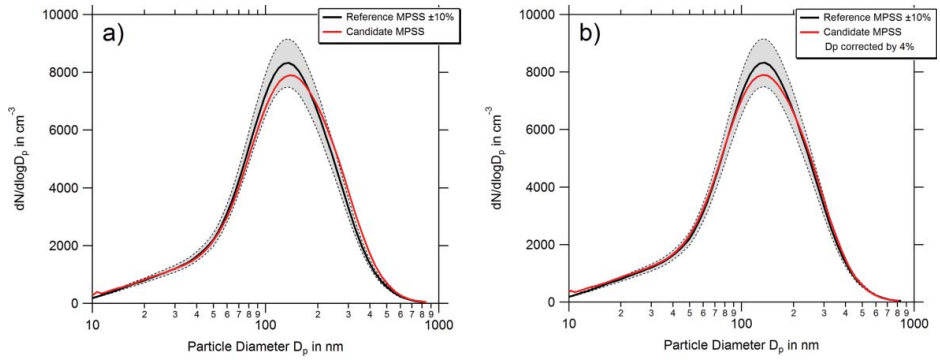

Figure 10. Intercomparison of the PNSD of the candidate (red curve) against the reference MPSS (black curve). The PNSD of the candidate MPSS is within 10% against the reference over the size range from 20 to 200 nm and up to 20% above 200 nm (a). A slight shift of 4% in diameter of the candidate MPSS brings the uncertainty in PNSD back to the target uncertainty of 10% above 200 nm (b).

3.2.2. Soft X-ray

First, we used a brand-new soft X-ray bipolar charger (TSI model 3088). The measurements shown in Figure 14 originate from an ECAC workshop in which a new TSI MPSS was calibrated. The bipolar charge equilibrium of Tigges et al. (2015) was used for the soft X-ray charger in the inversion routine. As shown in Figure 14a, the PNSD of the candidate (soft-X-ray) is within the +/−10% target uncertainty compared to the PNSD of the reference MPSS (Kr^{85}). The integrated PNC of the candidate and reference MPSS are plotted against the PNC of the reference CPC in Figure 14b. Both comparisons, candidate (red dots) and reference MPSS (black dots) are clearly within the +/−10% target uncertainty. The comparison of an MPSS, using a brand-new soft X-ray bipolar charger, against a Kr^{85} bipolar diffusion charger was excellent.

Soft X-ray bipolar diffusion chargers seem thus to be a good choice, however, there might be also a limitation to their use due to possible altering effects. Unfortunately, a long-term investigation has yet to be done, studying effects, which might cause a creeping degradation of the performance. The manufacturer claims a guaranteed lifetime of approximately 8500 working hours. In the second step, we used a soft X-ray bipolar charger (model TSI 3087) with an operational time below 8500 working hours and with an "OK" status. Here, we employed the two reference MPSSs (#1 & #2), which were both operated with Kr85 bipolar diffusion charger in the first step. In the second step, #2 was operated with the used soft X-ray bipolar diffusion charger. Unfortunately, at this time, no reference CPC was available to determine the total PNC directly, so we could only compare the results of both MPSSs against each other. Figure 15a shows the comparison of the PNSD of both MPSSs (Soft X-ray in red and Kr^{85} in black). The PNSD determined with the X-ray bipolar diffusion charger is clearly outside of the +/−10% target uncertainty. While the comparison of the integrated PNC between the two MPSSs operated with Kr^{85} bipolar diffusion chargers is excellent (Figure 15b, black dots), the PNC of the MPSS operated with the X-ray bipolar diffusion charger is overestimated by 24% (right set of dots). The reason of this behavior is not clear. It might be that internal pollution

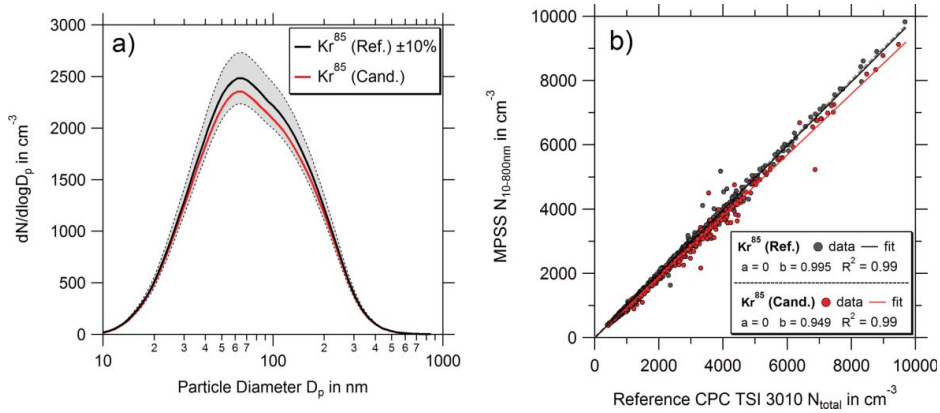

Figure 11. Intercomparison of two Kr^{85} (370 MBq) bipolar diffusion chargers. The PNSD of the candidate is within the +/−10% target uncertainty compared to the reference MPSS (a). The integrated PNC of the candidate and reference MPSS are within +/−10% uncertainty range against the reference CPC (b). Time resolution of the data is 10 min.

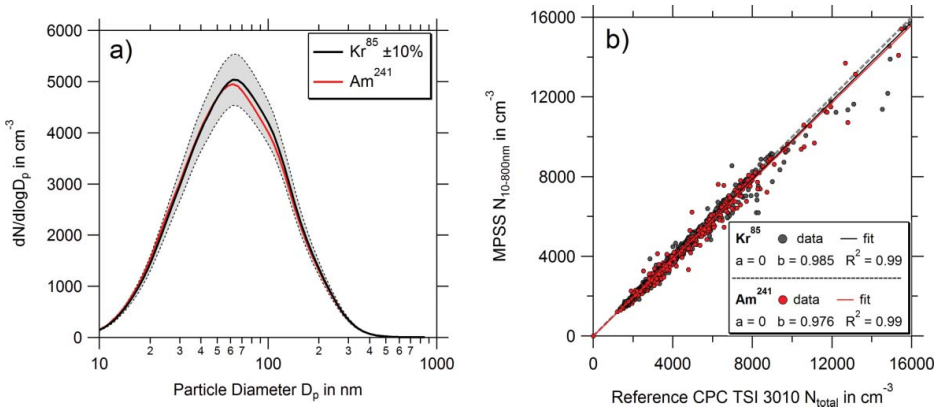

Figure 12. Intercomparison of a Kr^{85} (370 MBq) and a Am241 (74 MBq) bipolar diffusion charger. The PNSD of the candidate is within the +/−10% target uncertainty compared to the reference MPSS (a). The integrated PNC of the candidate and reference MPSS are within +/−10% uncertainty range against the reference CPC (b). Time resolution of the data is 10 min.

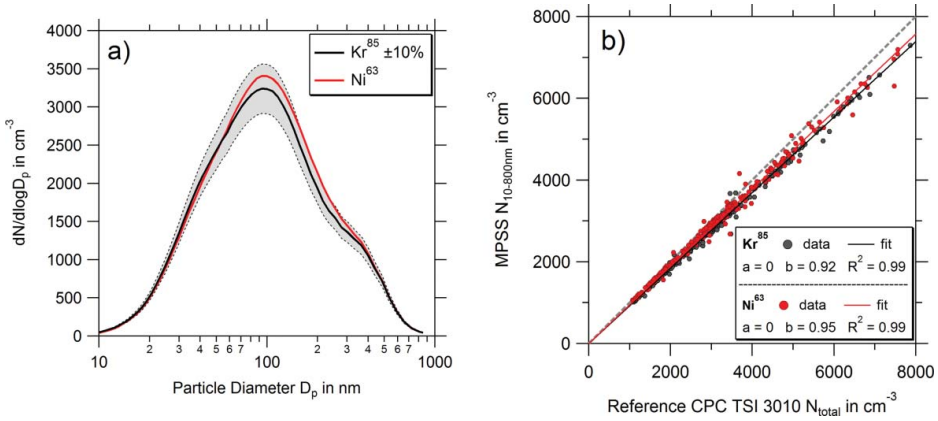

Figure 13. Intercomparison of a Kr^{85} (370 MBq) and a Ni63 (95 MBq) bipolar diffusion charger. The PNSD of the candidate is within the +/−10% target uncertainty compared to the reference MPSS (a). The integrated PNC of the candidate and reference MPSS are within +/−10% uncertainty range against the reference CPC (b). Time resolution of the data is 10 min.

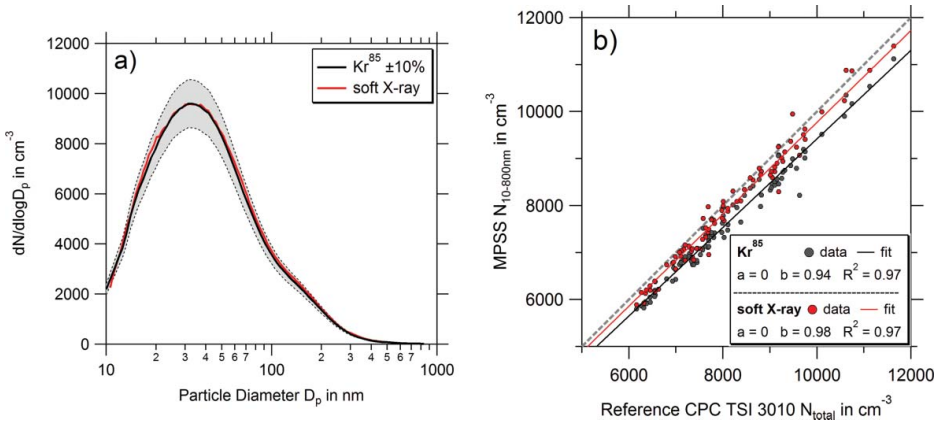

Figure 14. Intercomparison of a Kr^{85} (370 MBq) and brand-new soft X-ray bipolar diffusion charger (model TSI 3088). The PNSD of the candidate are within the +/−10% target uncertainty compared to the reference MPSS (a). The integrated PNC of the candidate and reference MPSS are plotted against the PNC of the reference CPC. Both comparisons, candidate (red dots) and reference MPSS (black dots) are clearly within the +/−10% target uncertainty. The time resolution of the data is 5 min.

causes a poor performance. We suggest, therefore, performing yearly calibrations of soft X-ray bipolar diffusion chargers. Additionally, a larger laboratory study should be done, investigating several soft X-ray bipolar diffusion chargers and their performance in terms of their age.

3.2.3. Electrical ionizer

To complete the analysis of different bipolar chargers, also the MSP electrical ionizer (model 1090) was tested (also denoted as TSI model 1090). This bipolar charger generates positive and negative ions by corona discharge. In this investigation, we used also a brand-new TSI version. As in the previous experiment (3.2.2), we used the two reference MPSSs (#1 and #2), #1 was operated with Kr^{85} bipolar diffusion charger and #2 with the electrical ionizer. Unfortunately, at this time, no reference CPC was available to determine the total PNC directly, so we could only compare the results of both MPSSs against each other. Figure 16a shows the comparison of the PNSDs of both MPSSs (electrical ionizer in red and Kr^{85} in black). The PNSD determined with the electrical ionizer is within the +/−10% target uncertainty. The comparison of the integrated PNC of the two MPSSs, one operated with the Kr^{85} bipolar diffusion charger and the other with the electrical ionizer, (Figure 16b, dots) are within the +/−10% target uncertainty, meaning that a new ionizer produces a bipolar charge equilibrium such as a Kr^{85} bipolar diffusion charger. Again, no long-term study on possible altering effects was performed so far. We suggest thus to observe the performance of the electrical ionizer by frequent calibrations.

3.3. Positive and negative DMA voltage

We also investigated the influence of a positive versus a negative DMA voltage in the MPSS, with respect to the uncertainty of the given negative and positive charge distribution (Wiedensohler 1988). For the laboratory set-up, we used two reference MPSSs (#1 and #2). For the first 8-h run, positive voltage power supplies were employed in both MPSSs (Figure 17). As shown in Figure 17b, the integrated PNC of the reference MPSS #2 was 5% higher compared to MPSS #1. This "system correction factor" of 1.05 between the two-reference MPSS is needed to correct the data of the second 8-h run. MPSS #1 and MPSS#2 used a positive and a negative high-voltage power supply, respectively. The results of this intercomparison run is shown in Figure 18. The PNSD of MPSS #2 was divided by the "system correction factor" of 1.05. The deviation between the PNSDs caused by using opposite polarity voltage is 10%. One can conclude that an MPSS using a negative voltage power supply underestimates the PNSD by approximately 10% compared to an MPSS using a positive voltage, if the same data processing is performed. This deviation is probably caused by uncertainties in the empirical data behind the approximation coefficients to calculate the bipolar charge distribution (Wiedensohler 1988). This deviation, however, is still within the target uncertainty of MPSS measurements.

Note: A positive DMA voltage is the default configuration in the reference MPSS and is used in all other tests and during normal operation.

3.4. Unipolarly precharged aerosol

The uncertainty in the PNSD that occurs using a unipolar precharged aerosol, as can be the case for laboratory-generated aerosol, depends on the performance

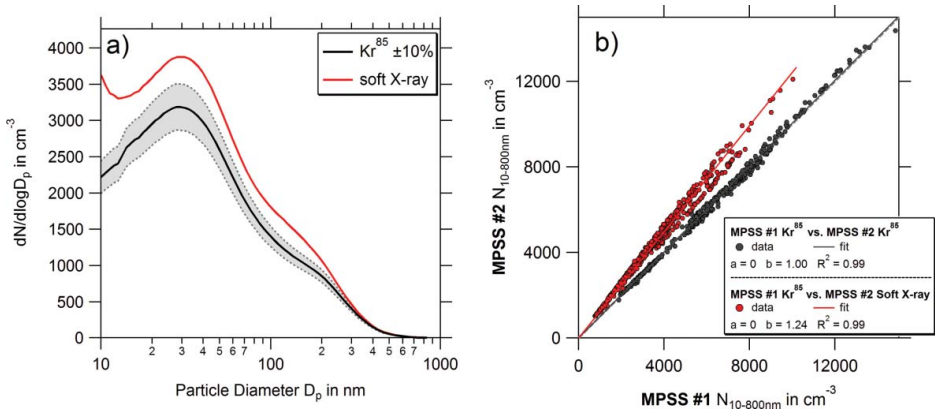

Figure 15. Intercomparison of a Kr^{85} (370 MBq) and a used soft X-ray bipolar diffusion charger (model TSI 3087). The PNSD of the candidate (soft X-ray in dark gray [red]) compared to the reference MPSS (Kr^{85} in black) is clearly outside of the +/−10% target uncertainty (a). Scatterplots of the integrated PNC of the two experiment are shown in b). While the comparison of the integrated PNC between the MPSS operated with Kr^{85} bipolar diffusion chargers is excellent (black dots), the PNC of the MPSS operated with the X-ray bipolar diffusion charger is overdetermined by 24% (right set of dots [red]). Time resolution of the data is 5 min.

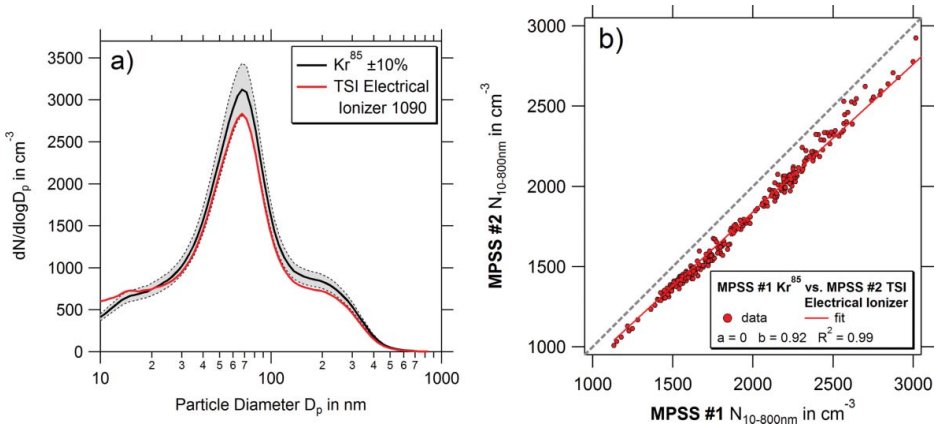

Figure 16. Intercomparison of a Kr^{85} (370 MBq) and electrical ionizer. The PNSD of the candidate MPSS (electrical ionizer in dark gray [red]) compared to the reference MPSS (Kr^{85} in black) is within the +/−10% target uncertainty over a wide range (a). The comparison of the integrated PNC of the two MPSSs, one operated with the Kr^{85} bipolar diffusion charger and the other with the electrical ionizer, (Figure 16b, dots [red]) are within the +/−10% target uncertainty (b). Time resolution of the data is 5 min.

of the bipolar diffusion charger. To test the performance of a reference MPSS with a Kr^{85} bipolar charger with 370 MBq, a nebulizer-generated ammonium sulfate aerosol is used, having an approximate geometric diameter of 100 nm and a geometric standard deviation of 2.0. We compared integrated PNCs up to 30,000 cm^{-3} against a reference CPC. The upper PNC was chosen to minimize errors due coincidence in the CPC (TSI model 3772). For this specific particle number size distributions (geometric mean diameter, geometric standard deviation and number concentration range), the specific bipolar diffusion charger was able to bring the unipolar precharged aerosol into the expected bipolar charge equilibrium (Wiedensohler 1988) as shown in Figure 19. The deviation of 3% is within the target uncertainty range. For different particle number size distributions, e.g., with a larger geometric mean diameter, this results might not be valid.

3.5. Particle number size distribution measurements at low pressure

Atmospheric PNSD measurements are also performed at high altitude sites or onboard of aircrafts with low MPSS operating pressures. However, there is no proof that the commonly used bipolar charge distribution (Wiedensohler 1988) is also valid within an acceptable uncertainty range for reduced pressures. In a first approximation, the bipolar charge equilibrium depends on the ratio of the mobility of negative and positive air ions. This ratio should remain constant for moderate pressure changes, meaning that the uncertainties of the given bipolar charge distribution and of the PNSD should not significantly increase. Because laboratory PNSD measurements at low pressure might risk unknown uncertainties, we used data from the atmospheric observatory at Chacaltaya, Bolivia, instead. The station is located at an altitude of

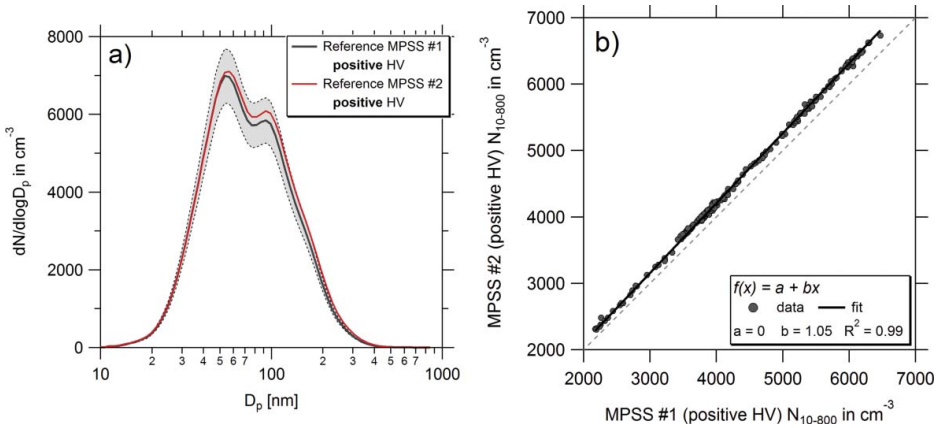

Figure 17. Intercomparison of two reference MPSSs (#1 and #2) using positive voltage power supplies. The integrated PNC of MPSS #2 is factor of 1.05 higher compared to reference MPSS #1.

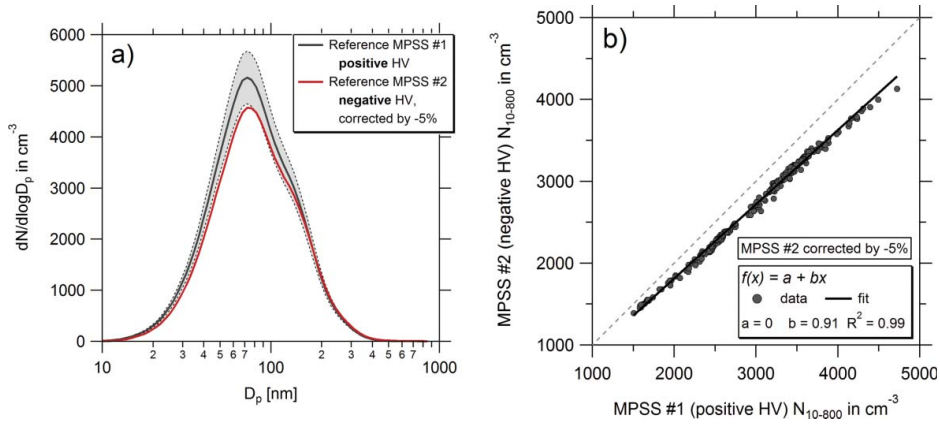

Figure 18. Intercomparison of two reference MPSSs (#1 and #2) using a positive and negative voltage power supply, respectively. The integrated PNC of MPSS #2 is corrected by a system correction factor of 1.05 (see Figure 17). The PNSD of MPSS #1 using a positive voltage power supply is 10% higher compared to MPSS #2 using a negative voltage power supply (left plot).

5240 m a.s.l. with an average ambient pressure of 540 hPa. PNSD and total PNC measurements are performed by an MPSS and a TSI CPC model 3772, respectively. In Figure 20, all valid PNSD and PNC data from the entire year 2014 are used to determine the uncertainty between the directly measured and integrated PNC. Only nighttime data from 12.00 PM to 06.00 AM have been used in order to exclude the influence of new particle formation during daytime. Although the measurements have not been taken under laboratory conditions, the slope is close to one and the data uncertainty is generally within the target of +/−10% with an acceptable R^2 of 0.93.

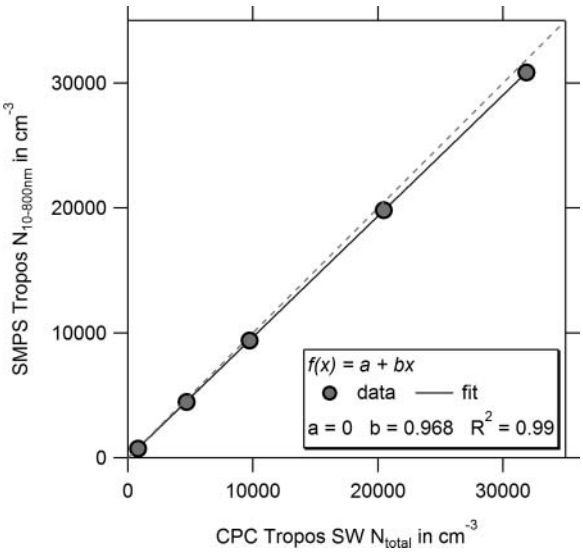

Figure 19. Intercomparison between the integrated PNCs and the directly measured number concentration of the reference CPC, using a laboratory-generated unipolarly precharged ammonium sulfate aerosol. The deviation of 3% is within the target uncertainty for PNCs.

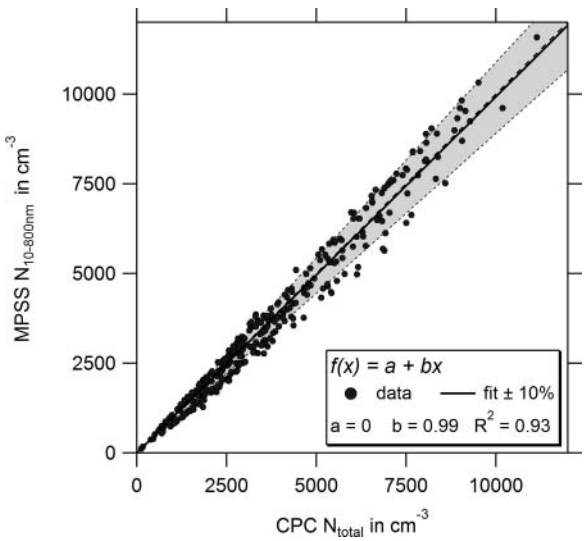

Figure 20. Scatterplot of the CPC-measured vs. the integrated PNC of ambient measurement at the Chacaltaya observatory, Bolivia, at a pressure of 540 hPa. The intercomparison shows a slope of close to one and the data are generally within the target uncertainty of +/−10% with a R^2 of 0.93. For this analysis, daily averages have been used.

4. Conclusions

To assure high quality of PNSDs measured by an MPSS, we recommend regular calibrations as done at ECAC/WCCAP for instruments from atmospheric observatories. The quality of the MPSS measurement strongly depends on the performance of the individual components and their interaction within the entire system. Consequently, regular quality assurance measures are needed to check the performance of an MPSS. However, only some parameters such as the particle size can be directly traced back to the SI, using a certified PSL particle size standard, preferably within the size range 100–350 nm. The sizing of particles generally relies on

knowledge of the Cunningham slip correction factor, whose values are agreed by convention and are not traceable. For particle number concentration (PNC) measurements, an SI-traceable aerosol electrometer can be employed to calibrate a condensation particle counter, which then can be used as a reference instrument. The determination of the PNSD is based on the commonly used equations for the bipolar charge equilibrium as described in ISO 15900, which is agreed by convention, and not traceable.

An MPSS calibration facility should have ideally one or several reference MPSSs and CPCs, which should undergo frequent calibrations (useful would be yearly). We propose the following procedures for a complete MPSS quality assurance program:

a) Calibration of the candidate CPC counting efficiency curve against a reference CPC or FCAE as described in ISO 27891
b) Sizing calibration of the candidate MPSS, using a certified polystyrene latex (PSL) particle size standard
c) Intercomparison of the PNSD of the candidate MPSS against a reference MPSS
d) Intercomparison of the integral PNC of the candidate MPSS against a calibrated reference CPC

All these procedures can either be traced back to SI units or related to conventions.

Based on the calibration of MPSSs at the European Center for Aerosol Calibration or the World Calibration Center for Aerosol Physics (ECAC/WCCAP; http://actris-ecac.eu/reports.html), we propose the following target uncertainty ranges for a candidate MPSS to pass the calibration successfully:

a) The PNC of the candidate CPC is within ±5% of that of the reference CPC in the size range of the plateau counting efficiency and the D_{P50} is within 1 nm to the nominal one.
b) The Particle sizing is within ±3% compared to the certified PSL particle size standard
c) The particle number size distribution of the candidate MPSS is within ±10% of that of the reference MPSS across the particle size range 20–200 nm (and within ±20% in the size range from 200 to 800 nm)
d) The PNC derived from the PNSD of the candidate MPSS is within ±10% of that of the reference CPC.

Based on calibration, field, and laboratory studies, we can further conclude:

a) Although specific unipolarly charged laboratory aerosols could be brought into the bipolar charge equilibrium under certain conditions, the best intercomparison results for PNC derived from MPSSs and CPCs might be achieved, when ambient air is used as calibration aerosol. This can be explained by the fact that the ambient aerosol tends to be already in a state close to the bipolar charge equilibrium.
b) An adjustment of the flow rate of the sheath air is useful to match the certified PSL particle size standard, even if the deviation is less than 3%. This will reduce deviations in terms of $dN/dlogD_P$ concentration in particle size range larger than 200 nm.
c) The choice of a bipolar diffusion charger based on the radioactive nuclide (Kr^{85}, Ni^{63}, Am^{241}) does not principally influence the performance of an MPSS for atmospheric measurements. Important is here that the actual activity of the radioactive sources is still sufficient. We did not include a bipolar diffusion charger based on Po210 in our investigation, since the half-life is only 138 days.
d) A brand-new soft X-ray charger performed well, according to the specific bipolar charge equilibrium. However, a device with working hours even below the recommended lifetime showed a significant degradation in its performance. An investigation of the long-term performance has to be done in future.
e) A brand-new bipolar diffusion charger based on corona discharge (called ionizer) performed well in preliminary tests. In addition, no studies have been done so far to quantify a possible degradation due to long-term altering of the corona discharger.
f) A positive power supply is recommended to use, if a choice can be made between positive and negative DMA voltage in an MPSS (i.e., measuring negatively charged particles). A 10% better agreement of the integral PNC with a reference CPC was achieved. Additionally, the fraction of negatively charged particles is generally greater than the one of positively charges particles, leading to better counting statistics in the measurements.
g) A PNSD can be confidently derived under conditions of low atmospheric pressure, such as found at high-altitude atmospheric observatories. Experimental results from the high-altitude station Chacaltaya, Bolivia (5240 m a.s.l.) confirm that the target uncertainty of ±10% in terms of PNC still can be met at atmospheric pressures as low as 500 hPa.

Acknowledgments

The authors would like to thank the Company TSI, Aachen, Germany, for their cooperation and fruitful discussion as well as for lending the electrical ionizer.

We would also like to thank Dr. Lucas Alados-Arboledas and his co-workers from Andalusian Institute for Earth System

Research (IISTA-CEAMA), University of Granada, Granada, Spain, to use results from their instrument in this study.

Funding

This work was accomplished in the frame of the project ACTRIS-2 (Aerosols, Clouds, and Trace gases Research InfraStructure) under the European Union—Research Infrastructure Action in the frame of the H2020 program for "Integrating and opening existing national and regional research infrastructures of European interest" under Grant Agreement N654109 (H2020—Horizon 2020).

Additionally, we acknowledge the WCCAP (World Calibration Centre for Aerosol Physics) as part of the WMO-GAW program base-funded by the German Federal Environmental Agency (Umweltbundesamt).

This work was supported by the EMPIR programme cofinanced by the Participating States and from the European Union's Horizon 2020 research and innovation programme. The work was done in the frame of the AEROMET project.

References

Agarwal, J. K. and Sem, G. J. (1980). Continuous Flow, Single-Particle-Counting Condensation Nucleaus Counter. *J. Aerosol Sci.*, 11:343–357.

Birmili, W., Stratmann, F., Wiedensohler, A., Covert, D., Russell, L. M., and Berg, O. (1997). Determination of Differential Mobility Analyzer Transfer Functions using Identical Instruments in Series. *Aerosol Sci. Technol.*, 27:215–223.

Brink ten, H., Plomp, A., Spoelstra, H., and van de Vate, J., (1983). A High Resolution Electrical Mobility Aerosol Spectrometer (MAS). *J. Aerosol Sci.*, 14:589–597.

Chen, D. R., Pui, D. Y. H., Hummes, D., Fissan, H., Quant, F. R., and Sem, G. J. (1998). Design and Evaluation of a Nanometer Aerosol Differential Mobility Analyzer (Nano-DMA). *J. Aerosol Sci.* 29:497–509.

Collins, D. R., Flagan, R. C., and Seinfeld, J. H. (2002). Improved Inversion of Scanning DMA data. *Aerosol Sci. Technol.*, 36:1–9.

Dahmann, D., Riediger, G., Schlatter, J., Wiedensohler, A., Carli, S., Graff, A., Grosser, M., Hojgr, M., Horn, H.-G., Jing, L., Matter, U., Monz, C., Mosimann, T., Stein, H., Wehner, B., and Wieser, U. (2001). Intercomparison of Mobility Particle Sizers (MPS). *Gefahrstoffe-Reinhaltung der Luft*, 61(10):423–428.

Gómez-Moreno, F. J., Alonso, E., Artíñano, B., Juncal-Bello, V., Iglesias-Samitier, S., Piñeiro Iglesias, M., López Mahía, P., Pérez, N., Pey, J., Ripoll, A., Alastuey, A., de la Morena, B A., Rodríguez, M I G., Sorribas, M., Titos, G., Lyamani, H., Alados-Arboledas, L., Latorre, E., Tritscher, T., and Bischof, O. F. (2015). Intercomparisons of Mobility Size Spectrometers and Condensation Particle Counters in the Frame of the Spanish Atmospheric Observational Aerosol Network, *Aerosol Sci. Technol.*, 49:777–785

Fissan, H., Helsper, C., and Thielen, H. (1983). Determination of Particle Size Distributions by Means of an Electrostatic Classifier. *J. Aerosol Sci.*, 14:354–357.

Flagan, R. (1999). On Differential Mobility Analyzer Resolution. *Aerosol Sci. Technol.*, 30:556–570

Fuchs, N. A. (1963). On the Stationary Charge Distribution on Aerosol Particles in a Bipolar Ionic Atmosphere. *Geofis. Pura. Appl.*, 56:185–193.

Hagwood, C., Sivathanu, Y., and Mulholland, G. (1999). The DMA Transfer Function with Brownian Motion a Trajectory/Monte-Carlo Approach. *Aerosol Sci. Technol.*, 30: 40–61.

Helsper, C., Horn, H. G., Schneider, F., Wehner, B., and Wiedensohler, A. (2008). Intercomparison of Five Mobility Size Spectrometers for Measuring Atmospheric Submicrometer Aerosol Particles. *Gefahrstoffe Reinhaltung der Luft.*, 68:475–481

Hermann, M., Wehner, B., Bischof, O., Han, H.-S., Krinke, T., Liu, W., Zerrath, A., and Wiedensohler, A. (2007). Particle Counting Efficiencies of New TSI Condensation Particle Counters. *J. Aerosol Sci.* 38:674–682.

Högström, R., Quincey, P., Sarantaridis, D., Lüönd, F., Nowak, A., Riccobono, F., Tuch, T., Sakurai, H., Owen, M., Heinonen, M., Keskinen, J., and Yli-Ojanperä, J. (2014). First Comprehensive Inter-Comparison of Aerosol Electrometers for Particle Sizes up to 200 nm and Concentration Range 1000 cm^{-3} to 17,000 cm^{-3}. *Metrologia*, 51:293–303.

Hoppel, W. (1978). Determination of the Aerosol Size Distribution from the Mobility Distribution of the Charged Fraction of Aerosols. *J. Aerosol Sci.*, 9:41–54.

Khlystov, A., Kos, G. P. A, ten Brink, H. M, Mirme, A., Tuch, T., Roth, C., and Kreyling, W. G. (2001). Comparability of Three Spectrometers for Monitoring Urban Aerosol. *Atmos. Environm.*, 35:2045–2051.

Knutson, E. O. and Whitby, K. T. (1975). Aerosol Classification by Electric Mobility: Apparatus, Theory and Applications. *J. Aerosol Sci.*, 6:443–451.

Kousaka, Y., Okuyama, K., and Adachi, M. (1985). Determination of Particle Size Distribution of Ultrafine Aerosols Using a Differential Mobility Analyzer. *Aerosol Sci. Technol.*, 4:209–225.

Liu, B. Y. H. and Pui, D. Y. H. (1974). Submicron Aerosol Standard and Primary, Absolute Calibration of the Condensation Nuclei Counter. *J. Colloid Interf. Sci.*, 47:155–171.

Pfeifer, S., Birmili, W., Schladitz, A., Müller, T., Nowak, A., and Wiedensohler, A. (2014). A Fast and Easy-to-Implement Inversion Algorithm for Mobility Particle Size Spectrometers Considering Particle Number Size Distribution Information Outside of the Detection Range. *AMT*, 7:95–105.

Russell, L. M., Flagan, R. C., and Seinfeld, J. H. (1995). Asymmetric Instrument Response Resulting from Mixing Effects in Accelerated DMA-CPC Measurements. *Aerosol Sci. Technol.*, 23:491–509.

Scheibel, H. and Porstendörfer, J. (1983). Generation of Monodisperse Ag- and NaCl-aerosols with Particle Diameters Between 2 and 300 nm. *J. Aerosol Sci.*, 14:113–126.

Stolzenburg, M. (1988). An Ultrafine Aerosol Size Distribution Measuring System. PhD thesis, Mechanical Engineering Department, University of Minnesota, USA.

Stolzenburg, M. R. and McMurry, P. H. (1991). An Ultrafine Aerosol Condensation Nucleus Counter. *Aerosol Sci. Technol.*, 14:48–65.

Stolzenburg, M. R. and McMurry, P. H. (2008). Equations Governing Single and Tandem DMA Configurations and a New Lognormal Approximation to the Transfer Function. *Aerosol Sci. Technol.*, 42:421–432.

Tigges, L., Wiedensohler, A., Weinhold, K., Gandhi, J., and Schmid, H.-J. (2015). Bipolar Charge Distribution of a Soft X-Ray Diffusion Charger. *J. Aerosol Sci.*, 90:77–86.

Tuch, T., Weinhold, K., Merkel, M., Nowak, A., Klein, T., Quincey, P., Stolzenburg, M., and Wiedensohler, A. (2016). Dependence of CPC Cut-Off Diameter on Particle Morphology and Other Factors. *Aerosol Sci. Technol.*, 50 (4):331–338.

Wang, S. and Flagan, R. (1990). Scanning Electrical Mobility Spectrometer. *J. Aerosol Sci.*, 13:20.

Wiedensohler, A. (1988). An Approximation of the Bipolar Charge Distribution for Particles in the Submicron Size Range. *J. Aerosol Sci.*, 19:387–389.

Wiedensohler, A., Orsini, D., Covert, D. S., Coffmann, D., Cantrell, W., Havlicek, M., Brechtel, F. J., Russell, L. M., Weber, R. J., Gras, J., Hudson, J. G., and Litchy, M. (1997). Intercomparison Study of the Size-Dependent Counting Efficiency of 26 Condensation Particle Counters. *Aerosol Sci. Technol.*, 27:224–242.

Wiedensohler, A., Birmili, W., Nowak, A., Sonntag, A., Weinhold, K., Merkel, M., Wehner, B., Tuch, T., Pfeifer, S., Fiebig, M., Fjäraa, A. M., Asmi, E., Sellegri, K., Venzac, H., Villani, P., Laj, P., Aalto, P., Ogren, J A., Swietlicki, E., Roldin, P., Williams, P., Quincey, P., Hüglin, C., Fierz-Schmidhauser, R., Gysel, M., Weingartner, E., Riccobono, F., Santos, S., Grüning, C., Faloon, K., Beddows, D., Harrison, R., Monahan, C., Jennings, S. G., O'Dowd, C., Marioni, A., Horn, H.-G., Keck, L., Jiang, J., Scheckman, J., McMurry, P. H., Deng, Z., Zhao, C. S., Moerman, M., Henzing, B., d. Leeuw, G., Löschau, G., and Bastian, S. (2012). Mobility Particle Size Spectrometers: Harmonization of Technical Standards and Data Structure to Facilitate High Quality Long-term Observations of Atmospheric Particle Number Size Distributions. *AMT*, 5:657–685.

Winklmayr, W., Reischl, G., Lindner, A., and Berner, A., (1991). A New Electromobility Spectrometer for the Measurement of Aerosol Size Distributions in the Size Range from 1 to 1000 nm. *J. Aerosol Sci.*, 22:289–296.

Zhang, S. H., and Flagan, R. C. (1996). Resolution of the Radial Differential Mobility Analyzer for Ultrafine Particles. *J. of Aerosol Sci.*, 27:1179–1200.